Journal of Science and Transport Technology
Journal homepage: https://jstt.vn/index.php/en

Investigation into the behavior of ballasted railway track foundations through numerical analysis

Nirmal Chandra Roy[1,2,*], Md. Abu Sayeed[2]
[1]Department of Civil Engineering, Hajee Mohammad Danesh Science and Technology University, Dinajpur, Bangladesh
[2]Department of Civil Engineering, Rajshahi University of Engineering and Technology, Rajshahi, Bangladesh

Article info
Type of article:
Original research paper

DOI:
https://doi.org/10.58845/jstt.utt.2025.en.5.3.61-70

***Corresponding author:**
Email address:
ncr.civil@hstu.ac.bd

Received: 21/4/2025
Received in Revised Form: 11/7/2025
Accepted: 24/7/2025

Abstract: Railways are now the most widely used form of public transport due to recent traffic congestion on highways in several countries worldwide, which has raised demand for quicker and larger trains. Modern railway traffic has led to the beginning of hefty wheel loads and high-speed trains, which has increased track layer stresses and resulted in excessive vibrations under dynamic loading. So, there is now a major rise in the risk linked to train operations in terms of train safety, track foundation degradation, and track damage. Studying how ballasted railway track foundations behave under various train speeds is essential to ensuring the dependability and safety of high-speed trains. The railway tracks were also stabilized with geo-grid to reduce the settlement of the track. This research paper presents a three-dimensional (3D) numerical approach to imitate the dynamic reaction to the ballasted railway's track subgrade systems for high-speed trains (HST). This study determined the time history curves for rail vertical displacement for the different elastic moduli of track layers. Also, the position of the geo-grid in the ballast layer (from 0.1 to 0.3 m) is investigated. Geo-grid stabilization can reduce about 24% vertical displacement for train dynamic load in the position of 0.1 m from the top of the ballast layer. The obtained results offer valuable insights into the dynamic reaction of ballast railway track subgrade systems, which can be utilized to enhance the design and maintenance of modern railways.

Keywords: Ballasted railway track; High speed train; Geo-grid; Displacement; Elastic modulus.

1. Introduction

Railways are now the most widely used form of public transport due to lately traffic congestion on highways in several countries worldwide, which has raised demand for quicker and larger trains. Recently, railway line had the potential to shift the current modal split, which is dominated by private (car or motorcycle) transportation customers [1]. Modern railway traffic has led to the beginning of hefty wheel loads and high-speed trains, which has increased track layer stresses and resulted in excessive vibrations under dynamic loading. Consequently, there is now a major rise in the risk link up with train operations in terms of train safety, track foundation degradation, fatigue failure of rails, and train power

supply interruption [2]. Contemporary railway traffic demands sophisticated design techniques for ballasted railway track foundations, which are required in order to reducing such dangers.

The components of a traditional ballasted railway track are the substructure (ballast, sub-ballast, and sub-grade) and the superstructure (rails, fastening system, and sleepers). The sleepers are evenly spaced over the length of the railway track to receive the wheel load from the rail. The sleepers attach the superstructure into the substructure layer and use a fastening technique to hold the rails in place. The stress induced at the contact area of ballast and sleeper is transferred to the sub-grade layer at a decreased level. An appropriate ballasted railway track system is needed to effectively reduce the stresses applied to the subgrade and avoid subgrade failure. When designing ballasted railway track foundations, the granular layer's thickness is taken into consideration [3]. The interactions between the rails, ties, ballast, and subgrade greatly influence the behavior of ballasted tracks. In addition to providing a stable support for the ties, the ballast layer also facilitates water drainage and absorbs the dynamic stresses created by passing trains [4]. According to an analysis of the stress distribution in ballast under train loads, the track's overall stability and serviceability are impacted by the high susceptibility of ballast particles to compaction and fragmentation [5]. While fine-grained ballast tends to produce increased compressive stress and earlier track degradation, well-graded ballast offers more constant load distribution and enhances track durability [6]. As the number of load cycles increases, the ballast's robust modulus decreases, resulting in long-lasting deformations [7]. One of the main issues with ballasted tracks is the track's progressive settling over time due to the cumulative effect of train loads. Excessive settlement may lead to misalignment and hazardous conditions [8]. Recent research has focused on using new technologies and alternative materials to improve the performance of ballasted tracks. The use of recycled materials, such as recycled broken concrete or rubber ballast, has been studied as a means of reducing costs and environmental impact. Recycled ballast materials can use less money and produce less waste while performing similarly to traditional ballast [9]. Geogrids are used in ballasted tracks to reduce the chance of track settlement and enhance load distribution [10].

To calculate the thickness of the granular layer, a variety of empirical and conceptually simple methods have been put out in the literature. These techniques include the UIC 719 R approach [11], the Canadian Modified approach [12], the British Rail method [13], the Japanese National Railways [14], and the American Railway Engineering Association (AREA) manual [15], in most of these design methodologies, the effect of the stiffness of each track layer was not considered, as all track layers were assumed to be a homogenous half- space in stress assessments. Moreover, the impact of recurrent loading on track settling was left out of the design parameters.

When a train travels on a railroad, the ballasted railway track elements become vulnerable to intricate loading, such as the rotation of the primary stress [16-19]. Accordingly, the degree of cumulative plastic strain and material stiffness may be impacted by train movement loads [20,21]. The dynamic influence of train movement loads cannot be adequately captured by current design methods. So, these methods are not appropriate for the demands of contemporary railway traffic [22,23].

Various numerical approaches, such as the boundary element method [24]; finite element method [25]; 2.5D FEM- Ground vibrations caused by trains have been predicted using BEM [26]. However, rather than taking into account actual (dynamic) moving loads, the majority of existing research examined a single cyclic or moving point load in order to examine the impact of train speed on track behavior and performance. It is exceedingly dubious to assume a single cyclic

load.

Recently, many researchers conducted 3D FE numerical modeling to calculate the induced stresses in the subgrade and ballast layers for different train speeds while taking dynamic amplification factors, which are impacted by the subgrade's properties into account [27-30]. Furthermore, as the train gets close to the critical speed, resonance can cause catastrophic track deflection [31]. Regretfully, there are no appropriate guidelines for taking the crucial speed into account when designing.

So, an advanced 3D FE modeling is produced to overcome the above limitations. The FE numerical simulation is a great substitute for field or laboratory testing because of the difficulties in substituting materials in various layers of the track sub-grade system. The creation of a 3D FEM for a typical ballast track sub-grade segment is the fundamental purpose of this investigation. The dynamic vertical displacement of the rail surface for different track sub-grade layers' elastic moduli.

2. Materials and Methods

In this investigation, the dynamic repercussion of ballasted railway track system sub-jugate to various train speeds and with different elastic modulus of sub-grade layers is superintended through a sophisticated 3D FE numerical modeling with the Midas-GTS commercial program [32]. The FE modeling and simulations are described in brief in this section.

2.1. Finite element model of railroad track foundations

In the numerical analysis track measurements taken into consideration are 36 m in long, 33 m in width and 12 m in deep. The model is created by extruding 3D meshes from 2D mesh. The elements of the track sub-grade system's cross-section are shown in Fig. 1, which serves as the foundation for creating the first 2D mesh. From this mesh, 3D meshes are extruded to represent different components, including a 0.3 m dense ballast layer, 0.2 m height sub-ballast layer, a 0.5 m capping layer, and 10.8 m deep soil layer. The 3D FE model's components are displayed in Fig. 2 as a 2D cross-sectional image that just contains quadrilateral shapes and leaves out triangular shapes. Tolerance restrictions are specified at 8 for aspect ratio, 45 for skew angle, 25 for warpage, and 0.25 for taper in order to ensure accuracy.

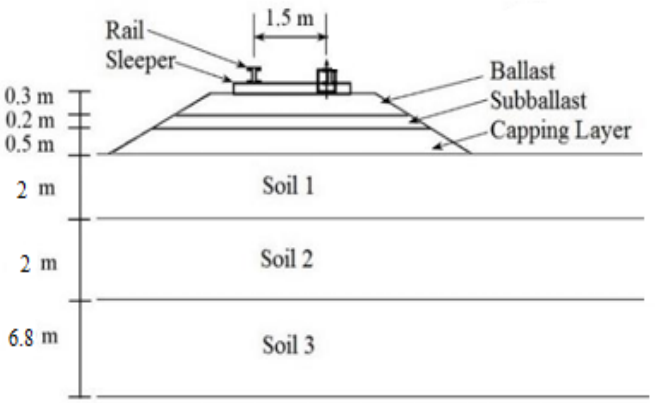

Fig. 1. Components of track sub-grade system

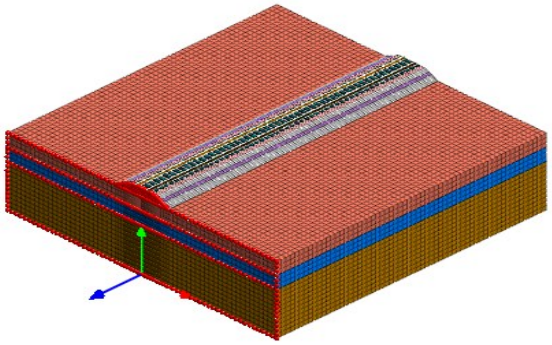

Fig. 2. 3D view of the model railway track system

A piece of one-dimensional (1D) I-beams that spans the track length is used to model the rail. It is assumed that the rail will have a section equivalent to the UIC-60 section. Rail pads, which fasten the rail to the sleepers, have an elastic stiffness link element equal to 100,000 kN/m. Based on the shortest wavelength required to accurately mimic high-frequency motion, the FE model's element size is estimated. Consequently, the 3D FE model's mesh sizes are the elements applied in the present investigation: 0.315 m × 0.14 m × 0.2 m for sleepers and 0.6 m × 0.6 m × 0.6 m for both ballast and sub-grade. There were 60 sleepers in all, spaced 0.6 m apart, along the line. The properties of rail, sleepers, and sub-grade were all represented as elastic materials and while

the ballast was modeled as an elasto-plastic Mohr-Coulomb material. A summary of each model material's attributes is provided in Table 1. Viscous dampers are used to join the model's vertical boundaries in order to replicate infinite boundary conditions and efficiently absorb incoming S- and P-waves. To replicate bedrock, the nodes at the bottom boundary were fixed in all directions. The tracks FE mesh consists of 181,210 elements and 180090 nodes. This study uses the Midas-GTS program to perform an eigenvalue analysis in order to confirm the 3D model's inherent frequency mode, accounting for the sub-grade response at the border of the multi- layer material mesh.

Table 1. Railway track model's material properties [33]

Material	Dynamic modulus, E (MPa)	Poisson's Ratio	Density (kN/m3)	Angle of Friction	Damping ratio
Ballast	400	0.10	17.7	50°	0.02
Sub-Ballast	300	0.02	21.6	40°	0.02
Capping Layer	200	0.02	21.6	36°	0.02
Soil-1	48	0.03	18.2	-	0.03
Soil-2	85	0.03	18.2	-	0.03
Soil-3	250	0.03	18.2	-	0.03
Sleeper	30000	0.20	20.2	-	-
Rail	210000	0.30	76.50	-	-

2.2. Simulation of train wheel loads

For the 3D FEM, a Thalys HST-type train is chosen to represent the HST moving load. The geometry of the Thalys HST including the carriage length (Lc), space between two bogies (L_b), space between axles (La) and wheel load (P) of each carriage are summarized in Table 2. The sleeper and rails have an element size of 0.315 m in the longitudinal direction. Therefore, a fastener spacing of 0.6 m is ensured by attaching the slab track to every other node of the rails. In this study, moving train load is simulated using the Midas-GTS software's dynamic load capability. The dynamic load table for an arbitrary node, with an axle load applied to each rail, is displayed in Fig. 3.

Table 2. Load patterns of Thalys HST [34]

Number of car	Length			Normal Wheel Load	
	L_a (m)	L_b(m)	L_c(m)	P_F(kN)	P_R(kN)
1	2.9	14.5	22.2	81	61.3
2	2.9	17.7	24.4	61.3	61.3
3	2.9	17.7	24.4	61.3	61.3
4	2.9	17.7	24.4	61.3	61.3
5	2.9	9.5	17.2	90	90

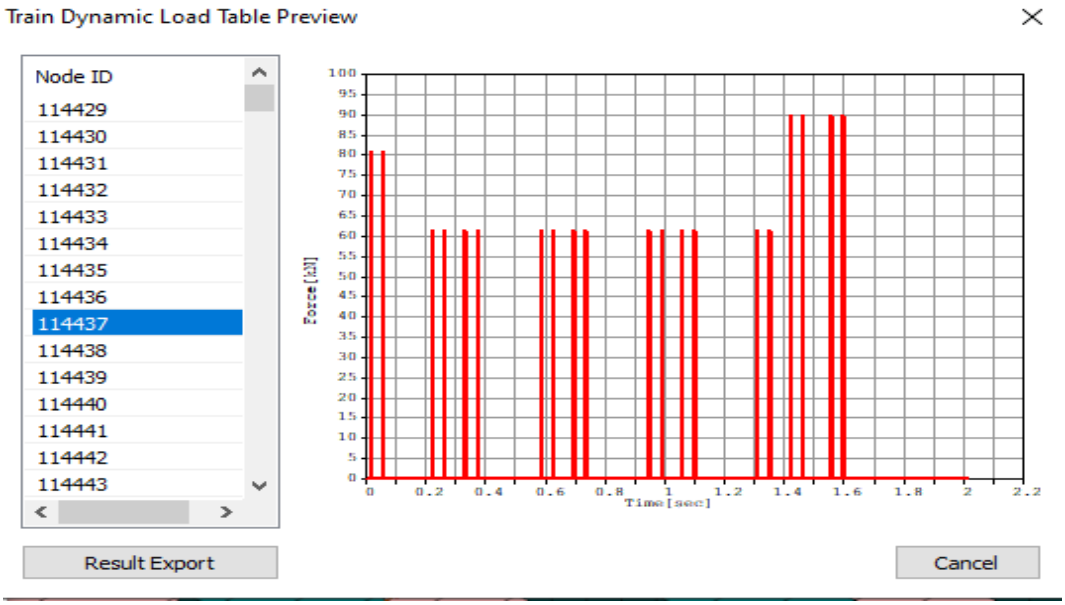

Fig. 3. Train dynamic load table (for 30 m/s speed)

2.3. Validation of the 3D FEM

To evaluate the precision and dependability of the 3D FEM, a rigorous validation procedure is used. The historical time responses of the sleeper displacement throughout the train's passage times were used to verify the FE modeling of the X-2000 HST railway track at Ledsgard site just outside Göteborg. Deflection of the track at Ledsgard site is measured physically for train speed of 70 km/h. Using Midas GTS program, at the track's center, the time-history responses of the sleeper deflection during the train's 70 km/h passing are computed. Next, the results are contrasted with the matching field measurements (for train speeds of 70 km/h) and the simulation response [35], as Fig. 4 illustrates (notice that positive values indicate upward deflections while negative values indicate downward deflections).

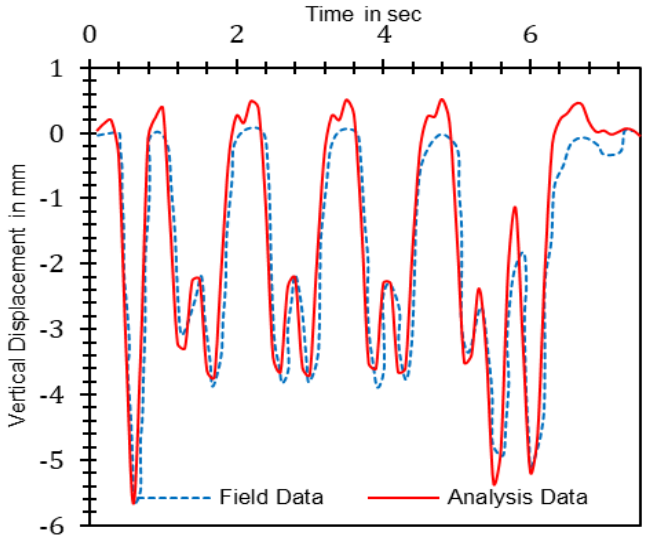

Fig. 4. Comparison of field observed and FE projected displacement responses at the track center

Although there are some small differences between physical model test measurements and the 3D FEM results, the comparison shows that the 3D FEM accurately represents the vertical displacement characteristics under train loading conditions. The physical model test results validation boosts the numerical analysis's accuracy and dependability confidence. To evaluate model performance and sensitivity some statical analysis tools are used. Root Mean Square Error (RMSE) and Coefficient of Determination (R^2) for curve similarity are carried out for field and analysis data.

$$RMSE=\sqrt{\frac{1}{N}\sum_{i=1}^{N}(A_i-F_i)^2} \quad (1)$$

$$R^2= 1-\frac{\sum(A_i-F_i)^2}{\sum(A_i-F)^2} \quad (2)$$

where, A_i= analysis data, F_i=field data

Equation (1) and (2) are used for RMSE and R^2 calculation and quantitative errors values are RMSE=0.6 mm and R^2=0.92 respectively. These indicate a very good match between the analysis and field data.

3. Result and Discussion

In these, current study the parameters which effects the ground track system is investigated using numerical analysis. The influencing parameters and their effects are summarized below-

3.1. Effect of Train speed

Train speed one of the most essential factors on which track performance depends. The sleeper's deflection of the railway track increases as the train velocity increases, and this occurs up to critical velocity. In Fig. 5, the deflection of the railway track caused by the train speed is shown which is measured below the sleeper.

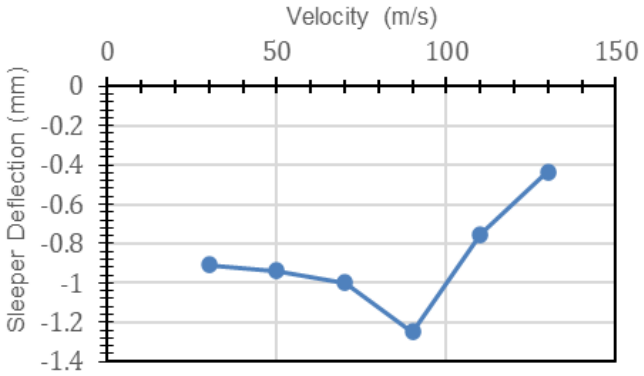

Fig. 5. Sleeper deflection with respective to train speed

After reaching critical speed about 90 m/s it shows maximum deflection and further increases speed of the train then vertical deflection is gradually decreased.

3.2. Effect of Elastic Modulus of the track materials

This part does parametric research to look into how the elastic modulus affects the vertical deflection of the rail. This is done using the same numerical model (Table 1) that was covered in the previous section. Nevertheless, just the relevant parameter is altered, as indicated in Table 3, in order to examine a particular parameter. Fig. 6 to Fig. 10 shows how the elastic modulus affects the vertical deflection of the track layer. It is evident that the vertical deflection of the rail is influenced by the elastic modulus of each track sub-structure layer. The shift in the sub-structure elastic modulus is the main cause of the fluctuation that has been seen.

In Fig. 6 shows that the variations of elastic modulus of the ballast materials affect the rail vertical displacement mostly. An increase of elastic modulus values the vertical displacement values decreases. Maximum vertical displacement value for train dynamic load is 1.8 mm, found for 135Mpa for train speed 30 ms^{-1}.

Table 3. Track attributes applied for the study

Parameter	Nominal Value of Dynamic Young's modulus, E (MPa)	Value Used at parametric study E (MPa)
Ballast	270	135, 400
Sub-Ballast	135	80, 300
Capping Layer	120	60, 200

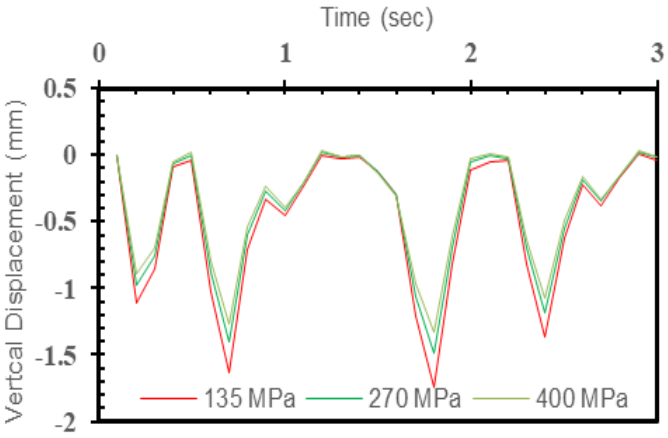

Fig. 6. Vertical displacement of rail for different elastic modulus of Ballast (30 ms-1)

In Fig. 7 shows the variation of vertical displacement of rail for different elastic modulus of ballast for the speed of 50 m/s.

In Fig. 8 shows the variation of vertical displacement of rail for different elastic modulus of ballast for the speed of 90 m/s.

The variations of elastic modulus of the ballast materials affect the track vertical displacement mostly as shown in Fig. 9. The vertical displacement values due to train dynamic load varies slightly for the $E = 135\,MPa$ to $E = 270\,MPa$. But further increases of elastic modulus values the vertical displacement values decreases. Maximum vertical displacement value for train dynamic load is 1.27 mm, found for 135Mpa.

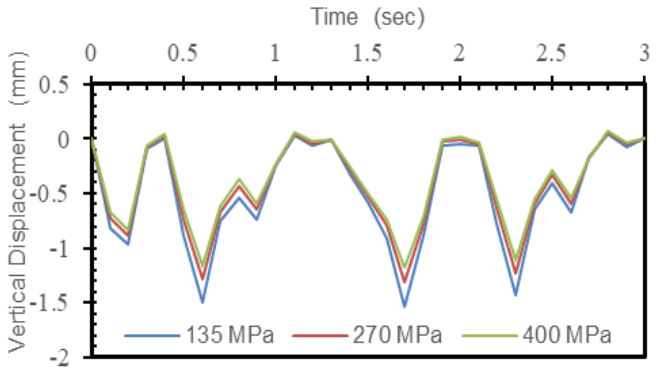

Fig. 7. Vertical displacement of rail for different elastic modulus of Ballast (50 ms^{1})

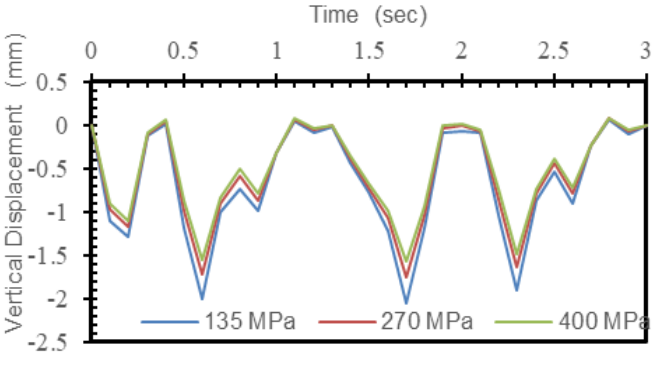

Fig. 8. Vertical displacement of rail for different elastic modulus of Ballast (90 ms^{-1})

In Fig. 10 shows the variations of elastic modulus of the sub-ballast layer affect the track vertical displacement mostly. An increase of elastic modulus values the vertical displacement values decreases. Maximum vertical displacement for

train dynamic load is 1.22 mm for elastic modulus 80 MPa.

Conversely, Fig. 11 to Fig. 14 shows that the vertical deflection is caused in the surrounding ground as well as close to the axle placements at the speed of 30 m/s for different time intervals.

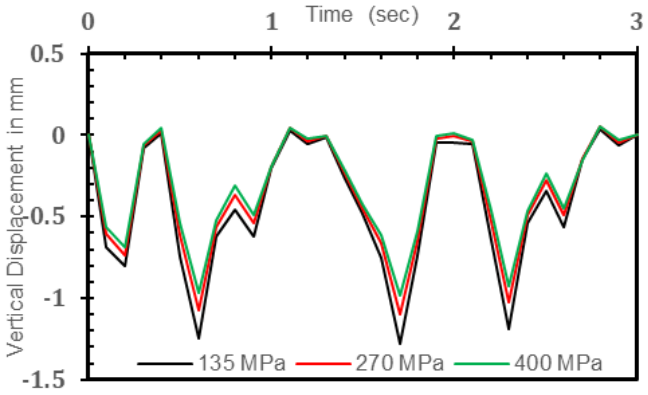

Fig. 9. Vertical displacement of ballast for different elastic modulus of Ballast

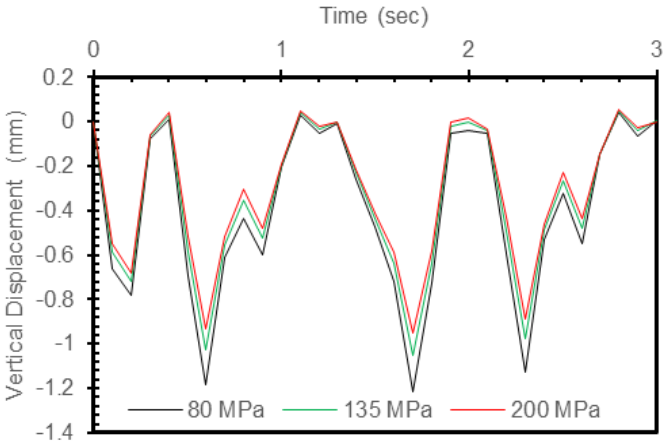

Fig. 10. Vertical displacement of Sub-ballast for different elastic modulus of Sub-Ballast

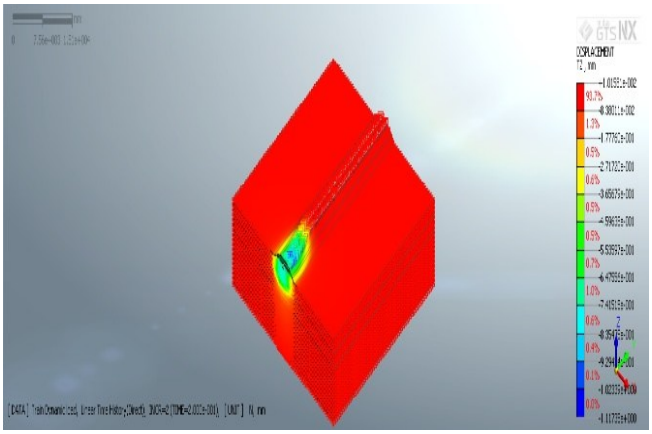

Fig. 11. Typical vertical track deflection contour plots for time interval 0.2 sec

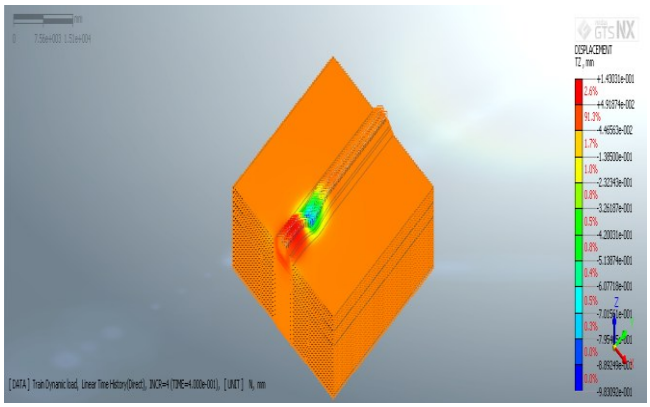

Fig. 12. Typical vertical track deflection contour plots for time interval 0.4 sec

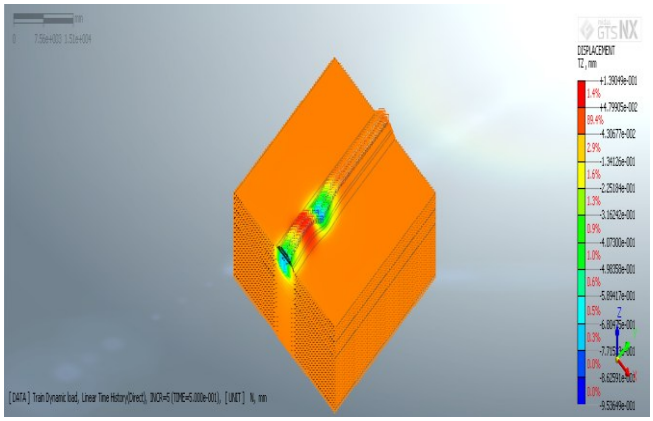

Fig. 13. Typical vertical track deflection contour plots for time interval 0.5 sec

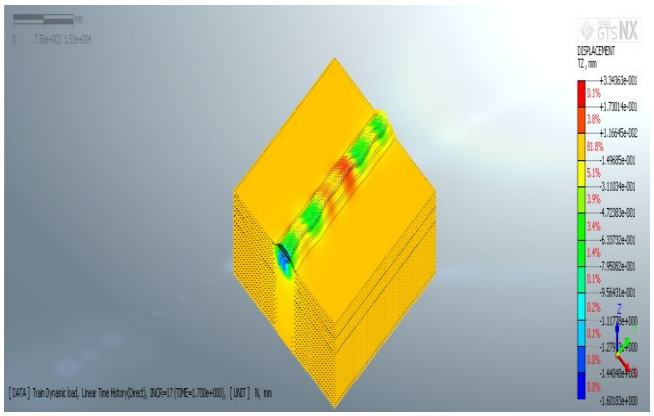

Fig. 14. Typical vertical track deflection contour plots for time interval 2.2 sec

3.3. Effect of Stabilizing Materials (Geo-grid)

The railway tracks behavior stabilized with geo-grid is also investigated. The railway tracks vertical displacement values can be reduced by different stabilizing materials such as geogrid, geotextiles, geocells. We consider geogrid as a stabilizing material. Properties of the geogrid that is used in the ballast layer are Material: HDPE or

PP (high-density polyethylene or polypropylene) Type: Biaxial or Triaxial geogrid Aperture size: 65 mm and thickness: 5 mm. The position of the geo-grid is varied to find out the suitable location where it can reduce maximum deflection of the railway track.

The effect of stabilizing materials such as geo-grid is shown in Fig. 15. By stabilizing the railway track with geo-grid, the vertical displacement values can be greatly decreased in the position of 0.1 m from top of the ballast layer. Railway track vertical displacement maximum value is 0.72 mm for dynamic load in normal conditions. But when the railway track is stabilized with geo-grid vertical displacement value is 0.55 mm in the same location which indicates geo-grid can be used significantly to decrease the displacement.

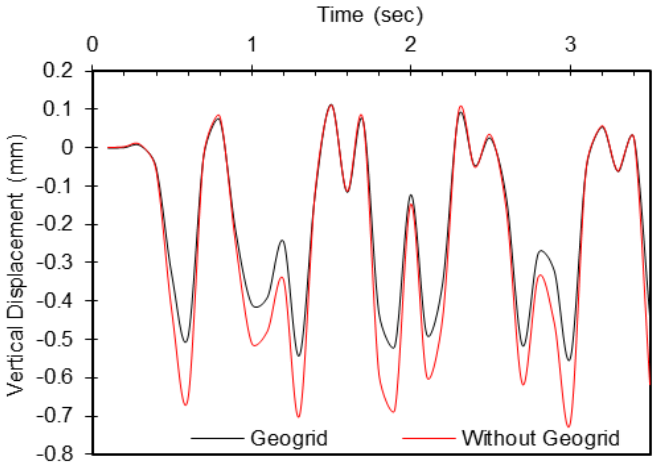

Fig. 15. Comparison of vertical displacement results without geo-grid and stabilized with geo-grid

4. Conclusions

In this research article, the dynamic response of a railway track system is thoroughly investigated numerically. The validation of the 3D FE model using a real model at full scale test demonstrates its accuracy in predicting the railway track system's dynamic reaction under HST movement conditions. The results of this investigation clearly show that the railway track system's overall displacement is influenced by the elastic modulus of the track materials and stabilizing materials. It is evident that a higher railway track layer elastic modulus and road bed results in a significant reduction in rail displacement and a smoother, more comfortable train ride. Geo-grid stabilization can reduce about 24% vertical displacement for train dynamic loads in the position of 0.1 m from the top of ballast layer which is 20% in the previous research works.

Acknowledgments

The authors want to acknowledge the Department of Civil Engineering, HSTU, Bangladesh, for their kind support and are thankful to the Department of Civil Engineering, RUET, Bangladesh, for the proper facilities.

References

[1]. T.T.M. Thanh, A.M. Ngoc. (2021). Urban Railway Development in Hanoi and the Possible Impacts on Mode Shifting: Experiences from Young Transport Users. *Journal of Science and Transport Technology*, 1(1), 9-23. https://doi.org/10.58845/jstt.utt.2021.en.1.1.9-23

[2] A.M. Kaynia, C. Madshus, P. Zackrisson. (2000). Ground vibration from high-speed trains: prediction and countermeasure. *Journal of Geotechnical and Geoenvironmental Engineering*, 126(6), 531-537. https://doi.org/10.1061/(ASCE)1090-0241(2000)126:6(531)

[3]. E.T. Selig, J.M. Waters. (1994). Track Geotechnology and Substructure Management. *Thomas Telford Publications, London, UK*. https://doi.org/10.1680/tgasm.20139

[4] A. Aikawa. (2013). Determination of dynamic ballast characteristics under transient impact loading. *Electronic Journal of Structural Engineering*, 13(1), 17-34. https://doi.org/10.56748/ejse.131581

[5] Z. Liu, B. Feng, E. Tutumluer. (2022). Effect of Ballast Degradation on Track Dynamic Behavior Using Discrete Element Modeling. *Transportation Research Record*, 2676(8), 452-462.

https://doi.org/10.1177/03611981221083921

[6] Y. Alabbasi, M. Hussein. (2021). Geomechanical Modelling of Railroad Ballast: A Review. *Archives of Computational Methods in Engineering*, 28, 815-839. https://doi.org/10.1007/s11831-019-09390-4

[7] B. Indraratna, D.J. Armaghani, A.G. Correia, H. Hunt, T. Ngo. (2023). Prediction of Resilient Modulus of Ballast Under Cyclic Loading Using Machine Learning Techniques. Transportation Geotechnics, 38, 100895. https://doi.org/10.1016/j.trgeo.2022.100895

[8] S. Fischer. (2025). Investigation of the Settlement Behavior of Ballasted Railway Tracks Due to Dynamic Loading. *Spectrum of Mechanical Engineering and Operational Research*, 2(1), 24-46. https://doi.org/10.31181/smeor21202528

[9] J. Jarjour, M. Meguid. (2023). On the Use of Recycled Waste Materials in Ballasted Railway Infrastructures: A Review. *Conference: Geosaskatoon 2023: Bridging infrastructures and resources, Canada*.

[10] P. Punetha, S. Nimbalkar. (2021). Performance Improvement of Ballasted Railway Tracks for High-Speed Rail Operations. *In: Barla, M., Di Donna, A., Sterpi, D. (eds) Challenges and Innovations in Geomechanics. IACMAG 2021. Lecture Notes in Civil Engineering, vol 126*. *Springer, Cham.* https://doi.org/10.1007/978-3-030-64518-2_100

[11] UIC. (1994). Earthworks and Trackbed Construction for Railway Lines, UIC Code 719 R. *International Union of Railways, Parish, France*.

[12]. G.P. Raymond. (1978). Design for railroad ballast and subgrade support. *Journal of the Geotechnical Engineering Division*, 104(1), 45-60. https://doi.org/10.1061/AJGEB6.0000576

[13] D.L. Heath, M.J. Shenton, R.W. Sparrow, J.M. Waters. (1972). Design of conventional rail track foundations. *Proceedings of the Institution of Civil Engineers*, 51(2), 251-267. https://doi.org/10.1680/iicep.1972.5952

[14] Z. Okabe. (1961). Laboratory investigation of railroad ballasts. *Bulletin of the Permanent Way Society of Japan*, 4(4), 1-19.

[15] AREA. (1996). Manual for Railway Engineering, Vol 1. *American Railway Engineering Association (AREA), Washington, D.C*.

[16] S.F. Brown. (1996). Soil mechanics in pavement engineering. *Géotechnique*, 46(3), 383-426. doi.org/10.1680/geot.1996.46.3.383

[17] W. Powrie, L.A. Yang, C.R.I. Clayton. (2007). Stress changes in the ground below ballasted railway track during train passage. *Proceedings of the Institution of Mechanical Engineers. Part F, Journal of Rail and Rapid Transit*, 221(2), 247-261. doi.org/10.1243/0954409JRRT95

[18] B. Dareeju, C. Gallage, T. Ishikawa, M. Dhanasekar. (2017). Effects of principal stress axis rotation on cyclic deformation characteristics of rail track subgrade materials. *Soils and Foundations*, 57(3), 423-438. doi.org/10.1016/j.sandf.2017.05.009

[19] P.J. Gräbe, C.R. Clayton. (2009). Effects of principal stress rotation on permanent deformation in rail track foundations. Journal of Geotechnical and Geoenvironmental Engineering, 135(4), 555-565. https://doi.org/10.1061/(ASCE)1090-0241(2009)135:4(555)

[20] A. Inam, T. Ishikawa, S. Miura. (2012). Effect of principal stress axis rotation on cyclic plastic deformation characteristics of unsaturated base course material. *Soils and Foundations*, 52(3), 465-480. doi.org/10.1016/j.sandf.2012.05.006

[21] J. Qian, Z. Du, X. Lu, X. Gu, M. Huang. (2019). Effects of principal stress rotation on stress–strain behaviors of saturated clay under traffic–load–induced stress path. *Soils and Foundations*, 59(1), 41-55. doi.org/10.1016/j.sandf.2018.08.014

[22] M.P.N. Burrow, D. Bowness, G.S. Ghataora. (2007). A comparison of railway track foundation design methods. *Proceedings of the Institution of Mechanical Engineers, Part F:*

Journal of Rail and Rapid Transit, 221(1), 1-12. doi.org/10.1243/09544097JRRT58

[23] P.J. Gräbe. (2002). Resilient and permanent deformation of railway foundations under principal stress rotation. *PhD Thesis, University of Southampton, Southampton, England*.

[24] Q. Sun, B. Indraratna, J. Grant. (2020). Numerical Simulation of the Dynamic Response of Ballasted Track Overlying a Tire-Reinforced Capping Layer. *Frontiers in Built Environment*, 6, 6, 1-15. doi.org/10.3389/fbuil.2020.00006

[25] A. El Kacimi, P.K. Woodward, O. Laghrouche, G. Medero. (2013). Time domain 3D finite element modelling of train-induced vibration at high speed. *Computers & Structures*, 118, 66-73. doi.org/10.1016/j.compstruc.2012.07.011

[26] X. Bian, C. Cheng, J. Jiang, R. Chen, Y. Chen. (2016). Numerical analysis of soil vibrations due to trains moving at critical speed. *Acta Geotechnica*, 11, 281-294. doi.org/10.1007/s11440-014-0323-2

[27] P. Alves Costa, R. Calçada, A. Silva Cardoso. (2012). Track-ground vibrations induced by railway traffic: In-situ measurements and validation of a 2.5D FEM-BEM model. *Soil Dynamics and Earthquake Engineering*, 32(1), 111-128. https://doi.org/10.1016/j.soildyn.2011.09.002

[28] P.A. Costa, A. Colaço, R. Calçada, A.S. Cardoso. (2015). Critical speed of railway tracks. Detailed and simplified approaches. *Transportation Geotechnics*, 2, 30-46. doi.org/10.1016/j.trgeo.2014.09.003

[29] M.A. Sayeed, M.A. Shahin. (2016). Three-dimensional numerical modelling of ballasted railway track foundations for high-speed trains with special reference to critical speed. *Transportation Geotechnics*, 6, 55-65. doi.org/10.1016/j.trgeo.2016.01.003

[30] H. Wang, L.-L. Zeng, X. Bian, Z.-S. Hong. (2020). Train moving load-induced vertical superimposed stress at ballasted railway tracks. *Advances in Civil Engineering*, 2020, 3428395. doi.org/10.1155/2020/3428395

[31] L.A. Yang, W. Powrie, J.A. Priest. (2009). Dynamic stress analysis of a ballasted railway track bed during train passage. *Journal of Geotechnical and Geoenvironmental Engineering*, 135(5), 680-689. doi.org/10.1061/(ASCE)GT.1943-5606.0000032

[32] MIDAS IT. Co. Ltd. (2013). Manual of GTS-NX 2013 v1.2: new experience of geotechnical analysis system. *MIDAS Company Limited, South Korea*.

[33] G. Degrande, L. Schillemans. (2001). Free field vibrations during the passage of a Thalys high-speed train at variable speed. *Journal of Sound and Vibration*, 247(1), 131-144. doi.org/10.1006/jsvi.2001.3718

[34] J. Cunha, A. Correia. (2012). Evaluation of a linear elastic 3D FEM to simulate rail track response under a high-speed train. *ICTG - Advances in Transportation Geotechnics II, Miura et al., eds., Taylor & Francis - Balkema, London, 196-201.*

[35] C. Madshus, A.M. Kaynia. (2000). High-speed railway lines on soft ground: dynamic behaviour at critical train speed. *Journal of Sound and Vibration*, 231(3), 689-701. doi.org/10.1006/jsvi.1999.2647